Chaos, Solitons & Fractals 44 (2011) 667–675

Contents lists available at ScienceDirect

Chaos, Solitons & Fractals

Nonlinear Science, and Nonequilibrium and Complex Phenomena

journal homepage: www.elsevier.com/locate/chaos

Bursting oscillations, bifurcation and synchronization in neuronal systems

Haixia Wang [a], Qingyun Wang [b,*], Qishao Lu [b]

[a] School of Science, Nanjing University of Science and Technology, Nanjing 210094, China
[b] Department of Dynamics and Control, Beihang University, Beijing 100191, China

ARTICLE INFO

Article history:
Received 28 March 2011
Accepted 1 June 2011
Available online 13 July 2011

ABSTRACT

This paper investigates bursting oscillations and related bifurcation in the modified Morris–Lecar neuron. It is shown that for some appropriate parameters, the modified Morris–Lecar neuron can exhibit two types of fast–slow bursters, that is "circle/fold cycle" bursting and "subHopf/homoclinic" bursting with class 1 and class 2 neural excitability, which have different neuro-computational properties. By means of the analysis of fast–slow dynamics and phase plane, we explore bifurcation mechanisms associated with the two types of bursters. Furthermore, the properties of some crucial bifurcation points, which can determine the type of the burster, are studied by the stability and bifurcation theory. In addition, we investigate the influence of the coupling strength on synchronization transition and the neural excitability in two electrically coupled bursters with the same bursting type. More interestingly, the multi-time-scale synchronization transition phenomenon is found as the coupling strength varies.

1. Introduction

Understanding the electrical properties of biological membranes in the single and populations of neurons is an important problem in computational neuroscience, which has attracted broad attention in the past several decades [1–3]. Neuronal firing behaviors can play important roles in neural encoding and information processing. For example, neural information is carried by various firing rhythm patterns and is contained in different spatio-temporal pulse patterns [1]. Some special bifurcation structure of the membrane potential may provide us with a clue to further understand mechanisms of neural encoding [4]. Synchronization may cause some neurological diseases such as epilepsy, essential tremor and Parkinson disease [5]. During the synchronization transitions, neural information can be transmitted from one neuron to others entirely or partially. Thus, different types of coupled bursters process information differently [6], and different synchronous regimes may correspond to different cognitive and pathological states [7].

Bursting oscillation has been extensively studied in neuronal models and other excitable cells. As a unit of neural information and the primary firing rhythm pattern, it involves two time scales with fast spiking and slow modulation. The experiments have shown that bursting can optimize insulin secretion in the pancreatic β-cells [8]. Bursting has more informational content and higher signal-to-noise ratio than the single spike [9]. Bursting oscillation is a prominent feature of cortical pyramidal cells and is thought to increase reliability of communication among neurons and synaptical plasticity [10,11]. It has also provided fertile ground for mathematical investigations on several levels, such as mathematical aspects of burster provided by Perc and Marhl [12], topological classification of bursters [2,6], and so on.

So far, many investigations have been made for analyzing dynamics of bursting oscillations, some important methods were proposed to uncover the bifurcation mechanism of transition between silent state and active state. The singular perturbation theory has been well developed since last century. Based on this, Wang et al. [13] investigated the asymptotic behavior of the Morris–Lecar (ML) model. Since the pioneering work of Rinzel [14] and the complete classification of point-cycle bursters firstly

* Corresponding author.
E-mail address: drwangqy@gmail.com (Q. Wang).

0960-0779/$ - see front matter © 2011 Elsevier Ltd. All rights reserved.
doi:10.1016/j.chaos.2011.06.003

provided by Hoppensteadt and Izhikevich [6,15], it has become a well accepted approach to study bursting oscillations by using fast–slow dynamics analysis. And the geometrical bifurcation analysis based on one-parameter and two-parameter bifurcation analysis is often used to investigate the generation or transition of bursting modes in the single neuron and bifurcation mechanisms of synchronized bursting in two-cell systems [16–25]. Tsaneva-Atanasova et al. [16] performed a detailed bifurcation analysis on the full fast–slow system of endocrine bursting models for square-wave and pseudo-plateau bursting patterns. Pernarowski [17] described dynamics of bursting and beating in a single cell by fast–slow dynamics analysis, and gave the asymptotic expansion of bursting solutions. Several modes of bursting in a Hodgkin–Huxley type neuronal model and transition of bursting in other models were studied in Refs. [18,19]. De Vries and Sherman [20] used the fast–slow dynamics analysis to investigate bifurcation mechanisms of emergent bursting in the single pancreatic beta cell and studied the dependence of bursting on the degree of heterogeneity and the coupling strength in two-cell system. Bertram et al. [21] studied bursting behavior in the Chay–Cook model with the two-parameter analysis. By means of two-parameter bifurcation analysis, Duan et al. [22] investigated the combined influences of the reversal potential of Ca^{2+} and the feedback current on the generation and transition of different bursting oscillations in the ML neuronal model with current-feedback. In addition, bifurcation mechanisms of bursting can also be understood by the unfolding and normal form theory [23–25].

Clinically, the connection between bursting and synchronization is extremely important, since synchronization in large neural populations is widely viewed as a hallmark of seizers. Burst synchronization may be influenced by many factors, such as coupling strengths, synaptic types, intrinsic dynamical feature and network topology. Belykh et al. studied the influence of coupling strength and network topology on bursting synchronization in networks of Hindmarsh–Rose neurons [26]. Batista et al. have studied the onset of phase synchronization on scale-free bursting neurons networks [27]. Bursting synchronization in inhibitorily coupled neurons has been studied and many interesting results were obtained. Synchronization on scale-free bursting neurons networks has been investigated [28–30]. The effects of the bifurcation structure of the coupled systems on synchronization have been investigated, where local divergence and slow passage effect were analyzed during synchronization, and some interesting results have been obtained [31,32]. A thorough analysis of the process of synchronization of bursting activity based on the calculation of the maximum transverse Lyapunov exponents has been preformed [33]. Furthermore, Shen et al. have studied burst synchronization in an ensemble of coupled Hindmash–Rose neurons [34]. In addition, synchronization transitions of complex neuronal networks have been recently investigated in detail as some key factors such as the information transmission delay, rewiring probability and network property are changed [35–38]. Some interesting results have been obtained, which can further elevate our understanding of synchronization in neuronal systems.

For further investigation of neuronal dynamics, we aim to explore bursting oscillators and corresponding bifurcations in the modified Morris–Lecar model. Two types of bursters are found as the key parameters are varied, and their generations are investigated in detail by means of the fast–slow dynamics analysis and bifurcation theory. At the same time, we study the synchronization of coupled bursting neurons. And then, complex bursting synchronization can be observed when the coupling strength is changed.

The present paper is arranged as follows. In Section 2, we introduce the model and explain two types of bursting in the single neuron for two parameters sets. In Section 3, we perform a detailed bifurcation analysis of the fast subsystem for two types of bursting patterns and explore the properties of some crucial bifurcation points by means of the stability and bifurcation theory. Section 4 shows synchronization transitions of two coupled bursters with the same type of bursting. Finally, the main conclusion is summarized in Section 5.

2. Model description

In this paper, we adopt the modified ML neuronal model [6,39], which is based on the famous two-dimensional Morris–Lecar model by changing the externally applied current I to be a slow linear feedback $a + bu$. Here, u is governed by a linear differential equation. Resultantly, the full system can be written as,

$$\dot{V} = -g_l(V - V_l) - g_k w(V - V_k) - g_{ca} m_\infty(V)(V - V_{ca}) + a + bu, \tag{1}$$

$$\dot{w} = \lambda(V)(w_\infty(V) - w), \tag{2}$$

$$\dot{u} = \mu(V + c). \tag{3}$$

where

$$m_\infty(V) = \frac{1}{2}\left(1 + \tanh\frac{V - v_1}{v_2}\right), \tag{4}$$

$$w_\infty(V) = \frac{1}{2}\left(1 + \tanh\frac{V - v_3}{v_4}\right), \tag{5}$$

$$\lambda(V) = \frac{1}{3}\cosh\frac{V - v_3}{2v_4}, \tag{6}$$

$$v_3 = d + eu. \tag{7}$$

The modified ML neuronal model can exhibit rich firing rhythm patterns as the parameter varies. This model is a multi-time-scale system characterized by two fast variables V, $w$and a slow adaptation current u. Here g_{ca}, g_k, g_l are the maximum conductance values for Ca^{2+}, K^+, and the leak pathways, respectively. V_{ca}, V_k, V_l are the equilibrium potentials corresponding to Ca^{2+}, K^+ and the leak conductance. Throughout the whole paper, we take $g_l = 0.5$ mmho/cm^2, $g_k = 2$ mmho/cm^2, $V_l = -0.5$ mV, $V_k = -0.7$ mV, $V_{ca} = 1$ mV, $v_1 = -0.01$ mV, $v_2 = 0.15$ mV. To investigate the bursting dynamics, we choose two sets of parameters as follows:

Case 1: $g_{ca} = 1.36$ mmho/cm^2, $a = 0$, $b = -1$, $c = 0.1$, $\mu = 0.005$, $d = 0.1$, $e = 0$, $v_4 = 0.16$ mV.

Case 2: $g_{ca} = 0.9$ mmho/cm^2, $a = 0.08$, $b = -0.03$, $c = 0.22$, $\mu = 0.003$, $d = 0.08$, $e = -1$, $v_4 = 0.04$ mV.

Fig. 1(a) and (b) shows the corresponding time series of the membrane potential V for two parameter sets, respectively. For convenience, we omit the unit of each variable in all figures. From Fig. 1, it can be found that the single neuron can exhibit different periodic bursting behaviors as the parameters are changed. Furthermore, two types of firing rhythm patterns can correspond to different bifurcation mechanisms and have different neuro-computational properties.

3. Bursting type analysis

Bursting is characteristic of multi-time-scale system. The neuron is said to be a fast–slow burster if its bursting behavior can be described by a singularly perturbed system of the following form

$$\dot{x} = f(x,y),$$
$$\dot{y} = \mu g(x,y),$$

where vector $x \in R^m$ describes relatively fast processes associated with spiking behavior, and $y \in R^k$ describes relatively slow processes that modulate fast spiking. $\mu \ll 1$ denotes the ratio of time scales between spiking and modulation. We refer to a burster as being planar if the fast spiking subsystem is two-dimensional. So far, twenty-four codimension one planar fast–slow bursters have been identified [6].

Firstly, we give an overview of fast–slow dynamics analysis, i.e. by decomposing the model into fast and slow subsystems, and then analyzing the dynamics of the full system in the limit of the slow variable treated as a bifurcation parameter. For Eqs. (1)–(3), since u is a slow variable, the full system can be decomposed into a fast subsystem (1) and (2) and a slow subsystem (3). By treating u as a bifurcation parameter, the steady state of fast subsystem obeys the following equations:

$$-g_l(V-V_l) - g_k w(V-V_k) - g_{ca} m_\infty(V)(V-V_{ca}) + a + bu = 0,$$
$$\lambda(V)(w_\infty(V) - w) = 0,$$

The u-nullcline satisfies:

$$\mu(V+c) = 0.$$

A burster can be defined by analyzing bifurcation mechanisms of steady state that transits from quiescence to repetitive spiking.

3.1. "Circle/fold cycle" bursting

In this section, we shall present the results of bifurcation and stability analysis on the single neuron based on Eqs. (1)–(7). By using MATCONT and PPLANE softwares [40,41], the bifurcations of fast subsystem for parameters Case 1 are shown in Fig. 2(a) and (b) with the slow variable u being treated as the bifurcation parameter. From Fig. 2(a), it is clear that there is a "Z"-shaped curve of steady state in (u,V)-plane. The curve is made up of three branches. On the upper branch, the equilibrium is either a stable focus or an unstable focus, whose stability changes via a subcritical Hopf bifurcation at point H with $u = -0.039234$. The erect lines represent the stable and unstable periodic orbits originating from the Hopf bifurcation point H, where the upper and lower endpoints of each line denote the maximum and minimum values of the corresponding periodic orbit. The points LP1 and LP2 with $u = 0.163901$ and $u = -0.07107$ represent fold bifurcation of equilibrium. The middle branch is made up of unstable saddles. On the lower branch, the equilibria are all stable nodes.

Fig. 2(b) is the enlargement of Fig. 2(a) with the trajectory of bursting being projected on the (u,V)-plane and the u-nullcline being superimposed. Since the u-nullcline is $V = -0.1$, below the slow nullcline, we have $\dot{u} < 0$. Hence, during the silent phase, the neuron follows the lower branch of equilibria to the left. At the left knee LP2, the unstable saddle and stable node merge into one, and then disappear. Meanwhile, a stable periodic orbit appears and goes through point LP2. The rest state switches to the repetitive spiking via the saddle-node bifurcation on the invariant circle (SNIC). Then u increases since $\dot{u} > 0$. When $u = -0.090766$, the stable and unstable periodic orbit coalesce and annihilate, i.e. fold bifurcation of limit cycle occurs, then the neuron is back to quiescence. Because the slow subsystem is driven by the fast variables, a hysteresis loop appears, which causes the alternation between two stable attractors. Hence, we can define this kind of burster

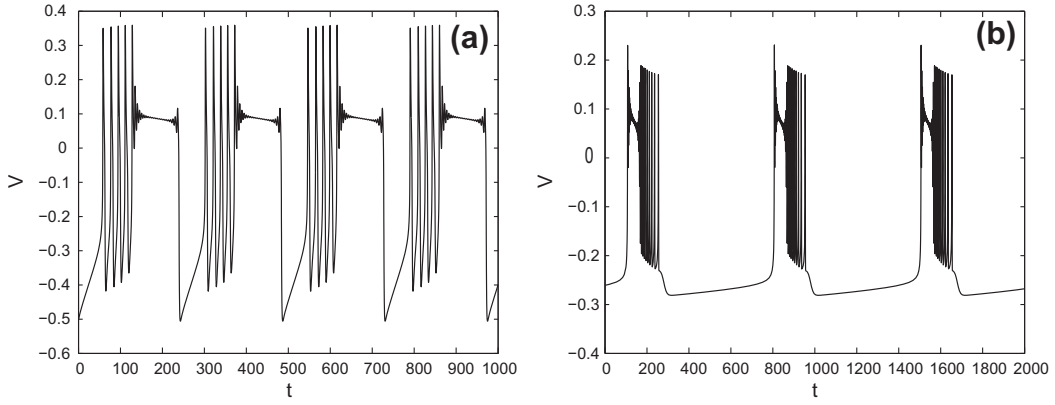

Fig. 1. The time evolution of the membrane potential V of the modified ML neuron for different sets of parameters (a) Case 1 and (b) Case 2.

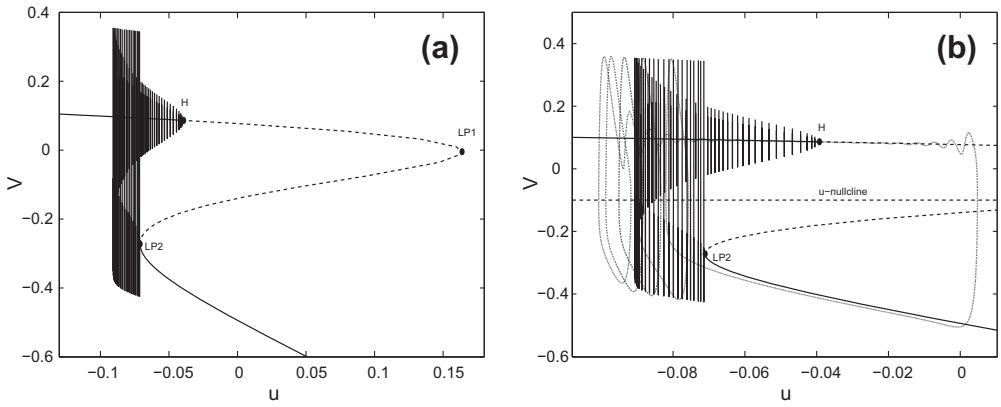

Fig. 2. (a) Bifurcation diagram of the fast subsystem with respect to the slow variable u, where H represents the subcritical Hopf bifurcation point, LP1 and LP2 represent the fold bifurcation points. On the "Z"-shaped curve of steady state, solid line denotes stable equilibria and dash line denotes unstable equilibria. (b) Enlargement of (a) with the trajectory of bursting (dot line) projected on the (u,V)-plane and the u-nullcline (dash line) superimposed.

as "circle/fold cycle" bursting with a "subHopf/fold cycle" hysteresis loop. Because the rest potential disappears through a saddle-node bifurcation on an invariant circle, this type of bursting belongs to class 1 neural excitability.

To understand the transition and bifurcation mechanisms associated with "circle/fold cycle" bursting, we show the phase portraits on (V,w)-plane in Fig. 3 with different values of u by means of the phase plane analysis. It is shown that when $u = -0.03$, the fast subsystem has a stable node, a saddle and an unstable focus, respectively. As u decreases to -0.05, the unstable focus becomes stable, and an unstable periodic orbit with the small amplitude appears. At that time, there exists a stable node and an unstable saddle in the fast subsystem. When $u = -0.07107$, an unstable saddle and a stable node merge into one point, and then annihilates each other. As a result, there exists a stable periodic orbit, which goes through the saddle-node and an unstable periodic orbit with small amplitude. Thus, the rest state transits to repetitive spiking via saddle-node bifurcation on the invariance circle. The hollow up-triangle represents the bifurcation point SNIC. As u exceeds the value $u = -0.07107$, for example we take $u = -0.078$, it is found that a stable and an unstable periodic orbit coexist with $u = -0.090766$ when fold bifurcation of limit cycle takes place. The stable and unstable limit cycle coalesce and annihilate. Hence, the neuron transits from repetitive spiking to rest state with a "subHopf/fold cycle" hysteresis loop. As u increases further, the fast subsystem only has a stable focus such as $u = -0.1$ shown in Fig. 3(f).

Secondly, we will testify properties of some important bifurcation points LP1, LP2 and H shown in Fig. 2(a), which

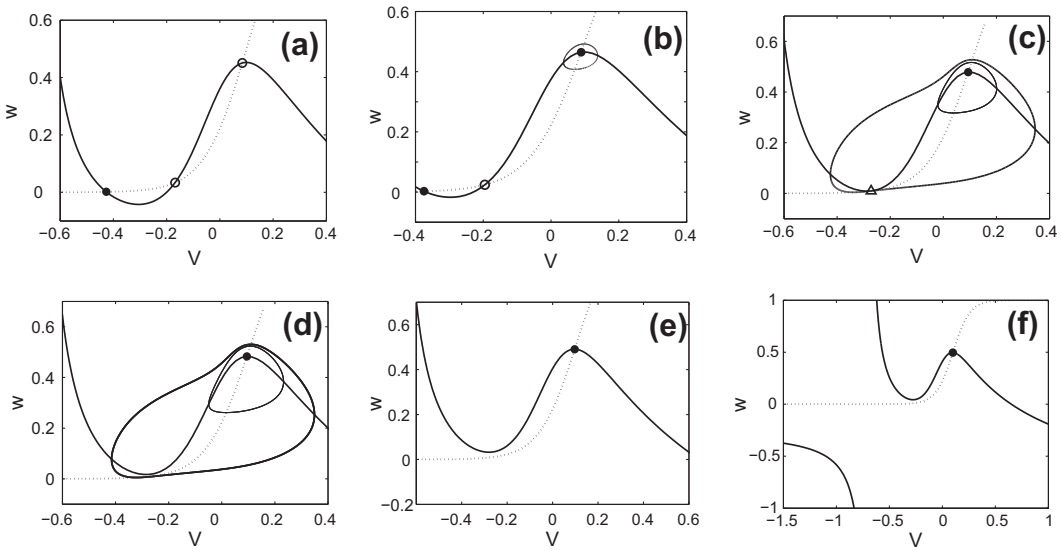

Fig. 3. The phase plane about (V,w) of the stable, unstable periodic orbits and V-nullcline (solid line), w-nullcline (dot line) for different u: (a) $u = -0.03$, (b) $u = -0.05$, (c) $u = -0.07107$, (d) $u = -0.078$, (e) $u = -0.090766$, (f) $u = -0.1$. Here the filled dot, hollow dot, hollow up-triangle, thin line and thick line represent the stable equilibrium, unstable equilibrium, bifurcation point, unstable and stable periodic orbit, respectively.

can determine the type of bursting. We calculate the first Lyapunov coefficient of the Hopf bifurcation point H to decide whether it is subcritical or supercritical or not [23,42]. For this purpose, we rewrite the fast subsystem (1) and (2) as,

$$\dot{V} = f_1(V, w, u), \tag{8}$$
$$\dot{w} = f_2(V, w, u), \tag{9}$$

where

$$f_1 = -g_l(V - V_l) - g_k w(V - V_k) - g_{ca} m_\infty(V)(V - V_{ca}) + a + bu, \tag{10}$$
$$f_2 = \lambda(V)(w_\infty(V) - w), \tag{11}$$

where $m_\infty(V)$, $w_\infty(V)$, $\lambda(V)$, v_3 are defined in Eqs. (4)–(7).

The Jacobian matrix can be written as

$$A = \begin{pmatrix} \frac{\partial f_1}{\partial V} & \frac{\partial f_1}{\partial w} \\ \frac{\partial f_2}{\partial V} & \frac{\partial f_2}{\partial w} \end{pmatrix},$$

where

$$\frac{\partial f_1}{\partial V} = -g_l - g_k w - g_{ca}\dot{m}_\infty(V)(V - V_{ca}) - g_{ca} m_\infty(V),$$
$$\frac{\partial f_1}{\partial w} = -g_k(V - V_k),$$
$$\frac{\partial f_2}{\partial V} = \dot{\lambda}(V)(w_\infty(V) - w) + \lambda(V)\dot{w}_\infty(V),$$
$$\frac{\partial f_2}{\partial w} = -\lambda(V),$$
$$\dot{m}_\infty(V) = \frac{2}{v_2\left(e^{\frac{V - v_1}{v_2}} + e^{-\frac{V - v_1}{v_2}}\right)^2},$$
$$\dot{w}_\infty(V) = \frac{2}{v_4\left(e^{\frac{V - v_3}{v_4}} + e^{-\frac{V - v_3}{v_4}}\right)^2},$$
$$\dot{\lambda}(V) = \frac{\left(e^{\frac{V - v_3}{2v_4}} - e^{-\frac{V - v_3}{2v_4}}\right)}{12 v_4}.$$

When $u = -0.07107$, the equilibrium of full system (1)–(3) is $(-0.27184, 0.0094898, -0.07107)$, the corresponding eigenvalues of Jacobian matrix A is $\lambda_1 \approx 0$, $\lambda_2 = -0.48463$. Meanwhile, there exists a stable limit cycle in the full system and the fast subsystem experiences the saddle-node bifurcation on invariance circle, i.e. LP2 is tested.

When $u = -0.039234$, the equilibrium of full system (1)–(3) is $(0.08623, 0.45735, -0.039234)$, the corresponding eigenvalues of Jacobian matrix A is $\lambda_{1,2} = \pm 1.2314i$. Hence, the Hopf bifurcation takes place in the fast subsystem.

When $u = 0.163901$, the equilibrium of full system (1)–(3) is $(-0.004484, 0.213148, 0.163901)$, the corresponding eigenvalues of Jacobian matrix A is $\lambda_1 = 2.5681$, $\lambda_2 \approx 0$. Hence, the fold bifurcation takes place in the fast subsystem, i.e. LP1 is tested.

In the following, we calculate the first Lyapunov coefficient at point H to decide whether it is a subcritical Hopf bifurcation point or not, for which the Jacobian matrix

$$A|_H = \begin{pmatrix} 0.3336 & -1.5726 \\ 1.0350 & -0.3336 \end{pmatrix}$$

with a simple pair of complex eigenvalues $\lambda, \bar{\lambda}$, with $\lambda = i\omega$, $\omega = 1.2314$. Let

$$q = \begin{pmatrix} 0.7766 \\ 0.1647 - 0.6081i \end{pmatrix} \in C^2$$

be a complex eigenvector corresponding to λ, which satisfies $Aq = i\omega q, A\bar{q} = -i\omega\bar{q}$, and the adjoint eigenvector

$$p = \begin{pmatrix} 0.6438 + 0.1745i \\ -0.8222i \end{pmatrix} \in C^2$$

has the properties $A^T p = -i\omega p, A^T\bar{p} = i\omega\bar{p}$, and satisfies the normalization condition $\langle p, q\rangle = 1$. Here $\langle p, q\rangle = \sum_{i=1}^{2}\bar{p}_i q_i$ is the standard scalar product in C^2.

Consider the system

$$\dot{x} = Ax + F(x), \quad x \in R^2,$$

where $F(x) = O(\|x\|^2)$ is a smooth function, A is the Jacobian matrix evaluated on the equilibrium. Write $F(x)$ in terms of multilinear functions $B(x,y)$, $C(x,y,z)$,

$$F(x) = \frac{1}{2}B(x,x) + \frac{1}{6}C(x,x,x) + O(\|x\|^4).$$

In coordinates, we have

$$B_i(x,y) = \sum_{j,k=1}^{2}\left.\frac{\partial^2 F_i(\xi)}{\partial\xi_j\partial\xi_k}\right|_{\xi=\xi_0} x_j y_k, \quad i = 1, 2,$$
$$C_i(x,y,z) = \sum_{j,k,l=1}^{2}\left.\frac{\partial^3 F_i(\xi)}{\partial\xi_j\partial\xi_k\partial\xi_l}\right|_{\xi=\xi_0} x_j y_k z_l, \quad i = 1, 2,$$

where $\xi = (\xi_1, \xi_2)^T$, ξ_0 is the equilibrium.

For the fast subsystem (8) and (9), we can write them as

$$\begin{pmatrix} \dot{V} \\ \dot{w} \end{pmatrix} = A|_H\begin{pmatrix} V \\ w \end{pmatrix} + \begin{pmatrix} F_1(V,w) \\ F_2(V,w) \end{pmatrix},$$

where

$$F_1(V,w) = 0.039234 - \frac{1}{2}(V + 0.5) - 2w(V + 0.7) - 1.36 m_\infty(V)(V - 1) - 0.3336V + 1.5726w,$$
$$F_2(V,w) = \lambda(V)(w_\infty(V) - w) - 1.035V + 0.3336w,$$
$$m_\infty(V) = \frac{1}{2}\left(1 + \tanh\frac{V + 0.01}{0.15}\right),$$
$$w_\infty(V) = \frac{1}{2}\left(1 + \tanh\frac{V - 0.1}{0.16}\right),$$
$$\lambda(V) = \frac{1}{3}\cosh\frac{V - 0.1}{0.32}.$$

Hence, we have

$$B(x,y) = \begin{pmatrix} -27.4093x_1y_1 - 2x_1y_2 \\ 0.8316x_1y_1 + 0.0448x_1y_2 \end{pmatrix},$$

$$C(x,y,z) = \begin{pmatrix} 59.962x_1y_1z_1 \\ -49.1944x_1y_1z_1 - 3.2582(x_1y_2z_1 + x_1y_1z_2 + x_2y_1z_1) \end{pmatrix}.$$

The first Lyapunov coefficient of H can be calculated by $l_1(0) = \frac{1}{2\omega} Re[\langle p, C(q,q,\bar{q}\rangle - 2\langle p, B(q, A^{-1}B(q,\bar{q}))\rangle + \langle p, B(\bar{q}, (2i\omega I - A)^{-1}B(q,q))\rangle]$. It follows that $l_1(0) = 36.532 > 0$. Hence the bifurcation point H is subcritical.

3.2. "SubHopf/homoclinic" bursting

For the second type of bursting shown in Fig. 1(b), the bifurcation diagram of fast subsystem with respect to the slow variable u is shown in Fig. 4. Fig. 4(b) is the enlargement of Fig. 4(a) with the trajectory of bursting projected on the (u,V)-plane and the u-nullcline $V = -0.22$ superimposed. It is clear that there is also a "Z"-shaped equilibria bifurcation curve in the (u,V)-plane with a slightly different shape from the former case. Three parts still exist: the upper branch is composed of focuses, the middle branch is composed of unstable saddle and the lower branch is composed of stable nodes. The separation of upper and middle branch is fold bifurcation point LP1 with $u = 0.175387$. The separation of middle and lower branch is another fold bifurcation point LP2 with $u = -0.033685$. On the upper branch, the rest potential loses stability via a subcritical Hopf bifurcation at H1 with $u = -0.013342$, which leads to transit from rest state to repetitive spiking. At about $u = -0.0229$, the stable and unstable periodic orbit coalesce and annihilate, and then fold bifurcation of limit cycle occurs. With the further increasing u, the spiking state reaches point H2, which is a saddle on the middle branch with $u = 0.0328$. Hence, a saddle homoclinic orbit forms, and the repetitive spiking switches to the rest state. This kind of bursting is defined as "subHopf/homoclinic" bursting with a "fold/fold" hysteresis loop. In addition, because the rest potential loses stability via Andronov–Hopf bifurcation, this type of bursting belongs to class 2 neural excitability.

Similarly, we may use the phase plane analysis to analyze properties of the equilibria and periodic orbit on the (V,w)-plane in Fig. 4 if we take some values of u.

It is shown in Fig. 5 that as $u = 0.1$, the fast subsystem has three equilibria, which are a stable node, a saddle and an unstable focus, respectively. As $u = -0.033685$, the unstable focus becomes stable, and no periodic orbit exists. However, the saddle and stable node merge into one point so that a fold bifurcation occurs in the fast subsystem. As $u = -0.03$, which is greater than -0.033685 and less than -0.0229, there exists a stable focus, a saddle and a stable node. For $u = -0.02$, a stable and unstable periodic orbit coexist with a stable focus, a saddle and a stable node. As u further increases to 0, the focus becomes unstable via subcritical Hopf bifurcation. When $u = 0.0328$, a homoclinic saddle orbit comes into being with a stable node and an unstable focus.

For the bifurcation points LP1, LP2 and H1 shown in Fig. 4(a), we can also verify their properties by calculating the Jacobian matrix evaluated on the corresponding points and obtain the following results.

When $u = 0.175387$, the equilibrium of full system (1)–(3) is $(-0.18646, 0.010436, 0.175387)$, and the corresponding eigenvalues of Jacobian matrix A are $\lambda_1 \approx 0$, $\lambda_2 = -0.043$. Hence, the fast subsystem experiences a fold bifurcation, i.e. LP1 is tested.

When $u = -0.013342$, the equilibrium of full system (1)–(3) is $(0.073692, 0.272396, -0.013342)$. The corresponding eigenvalues of Jacobian matrix A are $\lambda_{1,2} = \pm 2.269i$. Hence, the Hopf bifurcation takes place in the fast subsystem, i.e. H1 is tested.

When $u = -0.033685$, the equilibrium of full system (1)–(3) is $(-0.254967, 0, -0.033685)$. Thus, the corresponding eigenvalues of Jacobian matrix A are $\lambda_1 = 0$, $\lambda_2 = -16.7181$. As a result, a fold bifurcation takes place in the fast subsystem, i.e. LP2 is tested.

Nextly, we compute the first Lyapunov coefficient of H1, for which the Jacobian matrix

$$A|_{H1} = \begin{pmatrix} 0.3435 & -1.5474 \\ 3.4034 & -0.3434 \end{pmatrix}$$

with a simple pair of complex eigenvalues $\lambda, \bar{\lambda}$, and $\lambda = i\omega(\omega = 2.269)$. The complex eigenvector of matrix A corresponding to λ satisfying $Aq = i\omega q, A\bar{q} = -i\omega\bar{q}$ is

$$q = \begin{pmatrix} 0.0837 + 0.5528i \\ 0.8291 \end{pmatrix} \in C^2$$

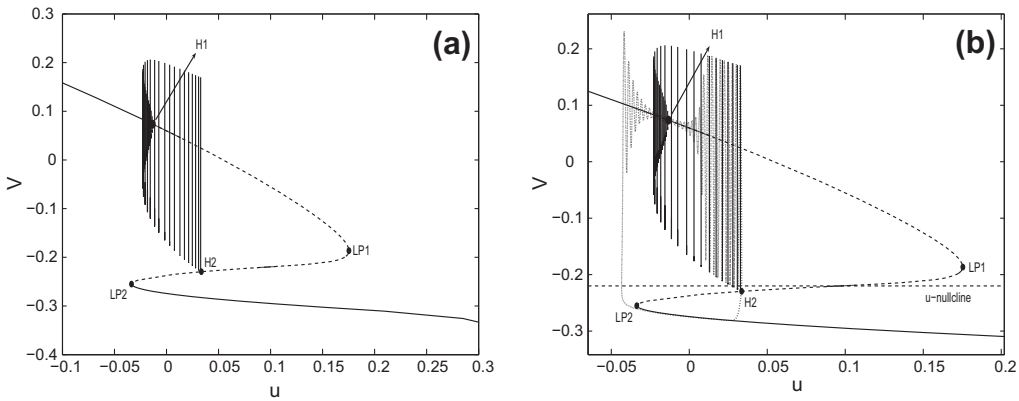

Fig. 4. (a) Bifurcation diagram of the fast subsystem with respect to the slow variable u, where H1 represents the subcritical Hopf bifurcation point and H2 represents the saddle, in which a homoclinic orbit forms. LP1 and LP2 are the fold bifurcation points. On the "Z"-shaped curve of steady state, solid line denotes stable equilibria and dash line denotes unstable equilibria. (b) Enlargement of (a) with the trajectory of bursting (dot line) being projected on the (u,V)-plane and the u-nullcline (dash line) being superimposed.

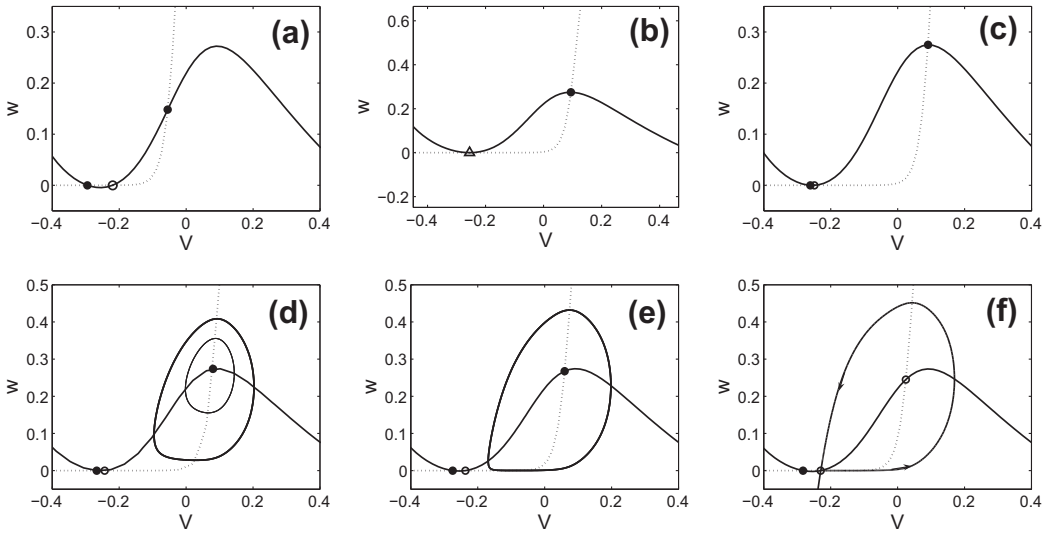

Fig. 5. The phase plane about (V,w) of the stable, unstable periodic orbits and V-nullcline (solid line), w-nullcline (dot line) with (a) $u = 0.1$, (b) $u = -0.033685$, (c) $u = -0.03$, (d) $u = -0.02$, (e) $u = 0$, (f) $u = 0.0328$. Where the filled dot, hollow dot, hollow up-triangle, thin line and thick line represent the stable equilibrium, unstable equilibrium, bifurcation point, unstable and stable periodic orbit, respectively. In (f), the arrow denotes the direction of the saddle homoclinic orbit.

and the adjoint eigenvector

$$p = \begin{pmatrix} 0.9044i \\ 0.603 - 0.0913i \end{pmatrix} \in C^2$$

has the properties $A^T p = -i\omega p, A^T \bar{p} = i\omega \bar{p}$, and the normalization condition $\langle p, q\rangle = 1$.

For the fast subsystem (8) and (9), we can write them as

$$\begin{pmatrix} \dot{V} \\ \dot{w} \end{pmatrix} = A|_{H1} \begin{pmatrix} V \\ w \end{pmatrix} + \begin{pmatrix} F_1(V,w) \\ F_2(V,w) \end{pmatrix},$$

where

$$F_1(V,w) = 0.0804 - \frac{1}{2}(V+0.5) - 2w(V+0.7) - 0.9m_\infty(V)(V-1) - (0.3435V - 1.5474w),$$

$$F_2(V,w) = \lambda(V)(w_\infty(V) - w) - (3.4034V - 0.3434w),$$

$$m_\infty(V) = \frac{1}{2}\left(1 + \tanh\frac{V+0.01}{0.15}\right),$$

$$w_\infty(V) = \frac{1}{2}\left(1 + \tanh\frac{V-0.09334}{0.04}\right),$$

$$\lambda(V) = \frac{1}{3}\cosh\frac{V-0.09334}{0.08}.$$

According to the expressions of $B_i(x,y)$ and $C_i(x,y,z)$, we can get

$$B(x,y) = \begin{pmatrix} -18.4131x_1y_1 - 2x_1y_2 \\ 56.9444x_1y_1 + 1.0315x_1y_2 \end{pmatrix},$$

$$C(x,y,z) = \begin{pmatrix} 2.8497x_1y_1z_1 \\ -721.3988x_1y_1z_1 - 53.6556(x_1y_2z_1 + x_1y_1z_2 + x_2y_1z_1) \end{pmatrix}.$$

The first Lyapunov coefficient of H1 is

$$l_1(0) = \frac{1}{2\omega} Re[\langle p, C(q,q,\bar{q}\rangle - 2\langle p, B(q, A^{-1}B(q,\bar{q}))\rangle + \langle p, B(\bar{q}, (2i\omega I - A)^{-1}B(q,q))\rangle] = 14.0694 > 0.$$

Hence, the Hopf bifurcation point H1 is also subcritical.

4. Synchronization transition of two coupled bursters

In what follows, we focus on synchronization transitions of two identical bursters coupled by electrical coupling. In particular, we investigate the influence of coupling strength on synchronization and neural excitability. The coupled neurons are governed by the following dynamical system,

$$\dot{V}_{1,2} = -g_l(V_{1,2} - V_l) - g_k w_{1,2}(V_{1,2} - V_k) - g_{ca1,ca2} m_{1\infty,2\infty}(V_{1,2} - V_{ca}) + a_{1,2} + b_{1,2}u_{1,2} + \sigma(V_{2,1} - V_{1,2}),$$

$$\dot{w}_{1,2} = \lambda_{1,2}(w_{1\infty,2\infty} - w_{1,2}),$$

$$\dot{u}_{1,2} = \mu_{1,2}(V_{1,2} + c_{1,2}),$$

where

$$m_{1\infty,2\infty} = \frac{1}{2}\left(1 + \tanh\frac{V_{1,2} - v_1}{v_2}\right),$$

$$w_{1\infty,2\infty} = \frac{1}{2}\left(1 + \tanh\frac{V_{1,2} - v_{31,32}}{v_{41,42}}\right),$$

$$\lambda_{1,2} = \frac{1}{3}\cosh\frac{V_{1,2} - v_{31,32}}{2v_{41,42}},$$

$$v_{31,32} = d_{1,2} + e_{1,2}u_{1,2}.$$

where, the subscripts 1,2 represent neuron 1 and neuron 2, respectively. Parameters g_l, g_k, V_l, V_k, V_{ca}, v_1, v_2 are taken the same values as the single neuron, and $\sigma > 0$ is the coupling strength.

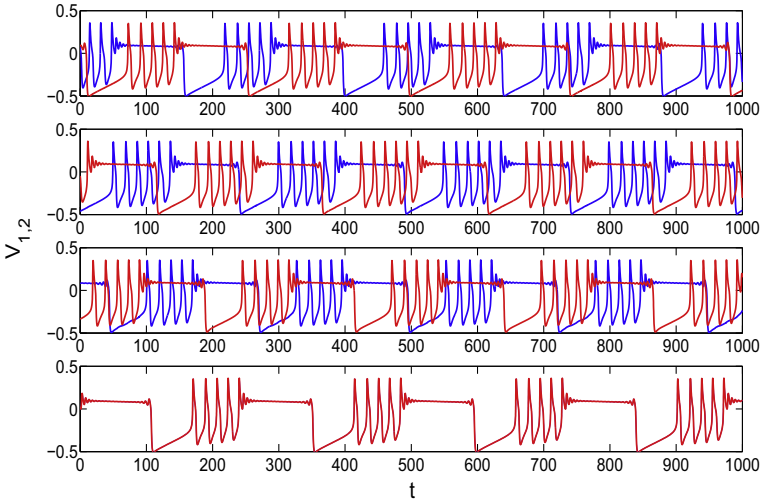

Fig. 6. The time evolution of two coupled "circle/fold cycle" bursters with different values of coupling strengths σ from top to bottom being $\sigma = 0.0001$, $\sigma = 0.003$, $\sigma = 0.007$, $\sigma = 0.01$, where the red and blue lines represent neuron 1 and neuron 2, respectively. (For interpretation of the references to colour in this figure legend, the reader is referred to the web version of this article.)

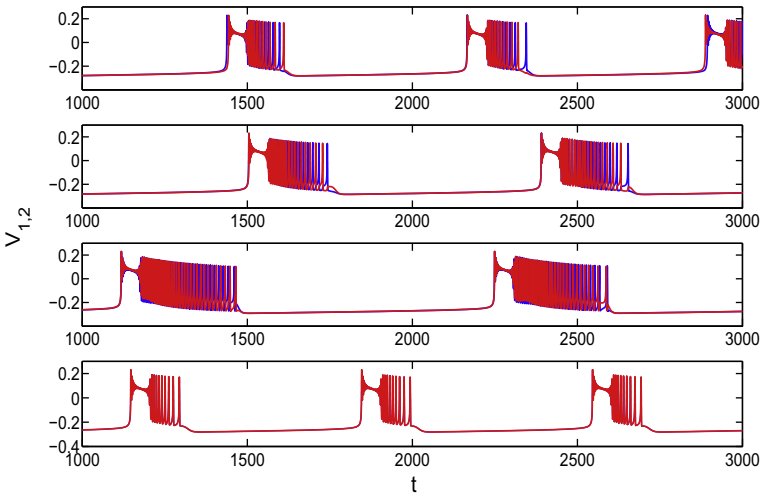

Fig. 7. The time evolution of two coupled "subHopf/homoclinic" bursters with different values of coupling strengths σ from top to bottom being $\sigma = 0.0001$, $\sigma = 0.03$, $\sigma = 0.1$, $\sigma = 0.13$, where the red and blue lines represent neuron 1 and neuron 2, respectively. (For interpretation of the references to colour in this figure legend, the reader is referred to the web version of this article.)

We consider two coupled identical bursters with the same type. Firstly, let neuron 1 and neuron 2 be "circle/fold cycle" burster. We take some typical values of coupling strength, synchronization transition in the coupled neurons can be shown in Fig. 6. It is observed that when the coupling strength is small, for example $\sigma = 0.0001$, two coupled bursters evolve independently. As coupling strength increases to $\sigma = 0.003$, a small correlation exists between two coupled bursters, and the number of spikes per burst changes from five to six. When the coupling strength increases to $\sigma = 0.007$, the correlation of two coupled bursters is further enhanced. Meanwhile, the number of spikes per burst turns back to the original state. As the coupling strength is big enough, for example $\sigma = 0.01$, two coupled bursters evolve coincidentally. Hence, complete synchronization takes place. During the whole process the type of burster is unaltered. However, the relative position and the number of spikes per burst change.

Nextly, we couple two identical "subHopf/homoclinic" bursters. The corresponding synchronization transition is illustrated in Fig. 7. It is observed that although the coupling strength is small, for example $\sigma = 0.0001$, two coupled bursters can obtain the burst synchronized state. When the coupling strength gradually increases, such as $\sigma = 0.03$ and $\sigma = 0.1$, the burst synchronization is still persisted although the number of spikes in each burst varies. As the coupling strength is large enough, two coupled bursters achieve a completely synchronized state, and the bursting behaviors are the same as those of the single neuron. Hence, for the two cases of electrically coupled bursters, we have found the multi-time-scale synchronization transition phenomenon, that is, due to the coupling, two

coupled bursters both transit from nonsynchronization to complete synchronization via burst phase synchronization. During the process, the type of each burster is unchanged. However, the number of spikes per burst varies slightly.

5. Conclusion

In this paper, we investigate the bifurcations associated with the bursting oscillations in the modified ML neuron and synchronization transitions of two coupled identical bursters. In particular, two types of bursters, which belong to "circle/fold cycle" bursting with class 1 neural excitability and "subHopf/homoclinic" bursting with class 2 neural excitability are found by means of fast–slow dynamics analysis and phase plane analysis. And then, dynamical characteristics of some crucial bifurcation points are verified by the stability and bifurcation theory. For two coupled identical modified ML bursters with the same bursting type and neural excitability, we have observed some interesting multi-time-scale synchronization transition phenomena as the coupling strength varies. In particular, as the coupling increases, two coupled bursters transit from nonsynchronization to complete synchronization via burst phase synchronization. More interestingly, during the process of synchronization transition, the type of each burster is unchanged with only the number of spikes per burst varying slightly. The results could be an important guidance for understanding dynamical behavior of neuronal system. Especially, interesting results of synchronization transition in the coupled bursters are a good supplement for our previous ones [35–38].

Acknowledgments

This work was supported by the National Science Foundation of China (Funds Nos. 11002073, 10972001, 10872014 and 10832006).

References

[1] Wulfram G, Werner MK. Spiking neuron models. Cambridge University Press; 2002.
[2] Izhikevich EM. Dynamical systems in neuroscience: the geometry of excitability and bursting. The MIT Press; 2005.
[3] Pikovsky A, Rosenblum M, Kurths J. Synchronization: a universal concept in nonlinear science. Cambridge University Press; 2001.
[4] González-Miranda JM. Block structured dynamics and neuronal coding. Phys Rev E 2005;72:051922.
[5] Milton J, Jung P. Epilepsy as a dynamic disease. Berlin: Springer; 2003. p . 1–14.
[6] Izhikevich EM. Neural excitability, spiking and bursting. Int J Bifurcation Chaos 2000;10:1171–266.
[7] Dzakpasu R, Zochowski M. Changes in synchrony and phase synchrony between individual neurons in normal and epileptic brain. Physica D 2005;208:115–22.
[8] Sato Y, Anello M, Henquin JC. Glucose regulation of insulin secretion independent of the opening or closure of adenosine triphosphate-sensitive K^+ channels in β cells. Endocrinology 1999;140:2252–7.
[9] Reinagel P, Godwin D, Sherman SM, Koch C. Encoding of visual information by LGN bursts. J Neurophysiol 1999;81:2558–69.
[10] Izhikevich EM. Bursts as a unit of neural information: selective communication via resonance. Trends Neurosci 2003;26:161–7.
[11] Huerta PT, Lisman JE. Bidirectional synaptic plasticity induced by a single burst during cholinergic theta oscillation in CA1 in vitro. Neuron 1995;15:1053–63.
[12] Perc M, Marhl M. Different types of bursting calcium oscillations in non-excitable cells. Chaos Solitons Fractals 2003;18:759–73.
[13] Wang J, Lu ML, Ye XW, Fei XY. Asymptotic behavior of Morris–Lecar system. Nonlinear Anal Real World Appl 2008;9:852–7.
[14] Rinzel J. Bursting oscillations in an excitable membrane model. New York: Springer-Verlag; 1985.
[15] Hoppensteadt FC, Izhikevich EM. Weakly connected neural networks. NY: Springer-Verlag; 1997.
[16] Tsaneva-Atanasova K, Osinga HM, Rieb T, Sherman A. Full system bifurcation analysis of endocrine bursting models. J Theor Biol 2010;264(4):1133–46.
[17] Pernarowski M. Fast subsystem bifurcations in strongly coupled heterogeneous collections of excitable cells. Bull Math Biol 1999;1:1–20.
[18] Shorten PR, Wall DJN. A Hodgkin–Huxley model exhibiting bursting oscillations. Bull Math Biol 2000;6(2):695–715.
[19] Yang ZQ, Lu QS. Different types of bursting in Chay neuronal model. Sci China Ser G-Phys Mech Astron 2008;51:687–98.
[20] De Vries G, Sherman A. From spikers to bursters via coupling: help from heterogeneity. Bull Math Biol 2001;63:371–91.
[21] Bertram R, Butte MJ, Kiemel T, Sherman A. Topological and phenomenological classification of bursting oscillations. Bull Math Biol 1995;57:413–39.
[22] Duan LX, Lu QS, Cheng DZ. Bursting of Morris–Lecar neuronal model with current-feedback control. Sci China Ser E: Technol Sci 2009;52:771–81.
[23] Kuznetsov Y. Elements of applied bifurcation theory. New York: Springer; 1995.
[24] Golubitsky M, Josic K, Kaper TJ. An unfolding theory approach to bursting in fast–slow systems in: global analysis of dynamical systems. J Physiol 2001:277–308.
[25] Azad AKA, Ashwin P. Within-burst synchrony changes for coupled elliptic bursters. SIAM J Appl Dyn Syst 2010;9:261–81.
[26] Belykh I, de Lange E, Hasler M. Synchronization of bursting neurons: what matters in the network topology. Phys Rev Lett 2005;94:188101.
[27] Batista CAS, Batista AM, de Pontes JAC, Viana RL, Lopes SR. Chaotic phase synchronization in scale-free networks of bursting neurons. Phys Rev E 2007;76:16218.
[28] Jalil S, Belykh I, Shilnikov A. Fast reciprocal inhibition can synchronize bursting neurons. Phys Rev E 2010;81(R):045201.
[29] Belykh I, Shilnikov A. When weak inhibition synchronizes strongly desynchronizing networks of bursting neurons. Phys Rev Lett 2008;101:078102.
[30] Belykh I, Jalil S, Shilnikov A. Burst-duration mechanism of in-phase bursting in inhibitory networks. Regular Chaotic Dyn 2010;15(2–3):148–60.
[31] Perc M, Marhl M. Local dissipation and coupling properties of cellular oscillators: a case study on calcium oscillations. Bioelectrochemistry 2004;62:1–10.
[32] Perc M, Marhl M. Synchronization of regular and chaotic oscillations: the role of local divergence and the slow passage effect. Int J Bifurcation Chaos 2004;14:2735–51.
[33] Dhamala M, Jirsa Viktor K, Ding MZ. Transitions to synchrony in coupled bursting neurons. Phys Rev Lett 2004;92:028101.
[34] Shen Y, Hou ZH, Xin HW. Transition to burst synchronization in coupled neuron networks. Phys Rev Lett 2008;77:031920.
[35] Wang QY, Duan ZS, Perc M, Chen GR. Synchronization transitions on small-world neuronal networks: effects of information transmission delay and rewiring probability. Europhys Lett 2008;83:50008.
[36] Wang QY, Duan ZS, Perc M, Chen GR. Synchronization transitions on scale-free neuronal networks due to finite information transmission delays. Phys Rev E 2009;80:026206.
[37] Wang QY, Chen GR, Perc M. Synchronous bursts on scale-free neuronal networks with attractive and repulsive coupling. PLoS One 2011;6(1):e15851.
[38] Wang QY, Aleksandra M, Perc M, Lu QS. Taming desynchronized bursting with delays in the Macaque cortical network. Chin Phys B 2011;20(4):040504.
[39] Wang HX, Lu QS, Wang QY. Bursting and synchronization transition in the coupled modified ML neurons. Commun Nonlinear Sci Numer Simul 2008;13:1668–75.
[40] Dhooge A, Govaerts W, Kuznetsov YuA. MATCONT: a MATLAB package for numerical bifurcation analysis of ODEs. ACM TOMS 2003;29:141–64.
[41] ODE software for MATLAB. Available from: http://math.rice.edu/dfield/.
[42] Sterpu M, Rocsoreanu C. Hopf bifurcation in a system of two coupled advertising oscillators. Nonlinear Anal: Real World Appl 2005;6:1–12.